RESEARCH ARTICLE

Key Points:

- Sedimentary delta[15]N and delta[98]Mo suggest less ventilated intermediate waters and more oxygenated bottom waters during early Holocene
- Reorganized subsurface circulation during mid-Holocene let to more oxygenated intermediate waters and anoxic bottom waters
- Weaker denitrification was associated with stronger summer monsoon and lower N_2O levels in the atmosphere

Supporting Information:

- Supporting Information S1

Correspondence to:
P. M. Kessarkar,
pratimak@nio.org

Variations in Denitrification and Ventilation Within the Arabian Sea Oxygen Minimum Zone During the Holocene

Pratima M. Kessarkar[1] , **S. W. A. Naqvi[1]**, **M. Thamban[2]**, **Lina L. Fernandes[1]**, **Christopher Siebert[3]**, **V. Purnachandra Rao[1,4]**, **H. Kawahata[5]** , **V. Ittekkot[6]** , and **Martin Frank[3]**

[1]CSIR-National Institute of Oceanography, Dona Paula, Goa, India, [2]National Centre for Antarctic and Ocean Research, Vasco da Gama, Goa, India, [3]GEOMAR Helmholtz Centre for Ocean Research Kiel, Kiel, Germany, [4]Department of Civil Engineering, Vignan's University, Vadlamudi, Guntur, India, [5]Ocean Research Institute, University of Tokyo, Tokyo, Japan, [6]University of Bremen, Bremen, Germany

Abstract The continental slope of India is exposed to an intense perennial oxygen minimum zone (OMZ) supporting pelagic denitrification. Sediments that are presently in contact with the lower boundary of the denitrification zone indicate marked changes in the intermediate and bottom waters ventilation of OMZ during the past 9,500 years. The $\delta^{15}N$ of sediment suggests that the OMZ waters were less ventilated during the early Holocene (between 9.5 and 8.5 ka BP) resulting in intensified denitrifying conditions with an average $\delta^{15}N$ value of 7.8‰, while at the same time stable Mo isotope composition (average $\delta^{98}Mo$ of −0.02‰) indicates that the bottom waters that were in contact with the sediments were better oxygenated. By the mid-Holocene OMZ became more oxygenated suppressing denitrification (average $\delta^{15}N$ of 6.2‰), while bottom waters gradually became less oxygenated (average $\delta^{98}Mo$ of 1.7‰). The mid-Holocene reduction in denitrification coincided with a global decrease in atmospheric N_2O as inferred from ice core records, which is consistent with a decreased contribution from the Arabian Sea. Since ~5.5 ka BP OMZ waters have again been undergoing progressive deoxygenation accompanied by increasing denitrification.

1. Introduction

The Arabian Sea is one of the three major oceanic areas where large-scale nitrogen loss occurs within well-defined mesopelagic oxygen minimum zones (OMZs), largely through denitrification (Codispoti et al., 2001; Naqvi, 1987). The OMZ of the Arabian Sea is today located between 100-/150- and 1,200-m depth (dissolved O_2 < 0.5 ml/L) and is the thickest of the global ocean (Sen Gupta & Naqvi, 1984; Wyrtki, 1971). In the upper part of the OMZ large deficits of nitrate (NO_3^-) are observed that are accompanied by accumulation of nitrite (NO_2^-) an intermediate of reduction of NO_3^- to N_2 (Devol et al., 2006). These NO_2^- bearing zones extend from the northwestern continental margin of India to the central Arabian Sea (Naqvi, 1991; Naqvi et al., 2003). Nitrate entrained from this zone into the surface layer in turn enriches the organic matter with ^{15}N, resulting in characteristically elevated $\delta^{15}N$ signatures of the organic matter preserved in the underlying sediments (Altabet et al., 1995, 2002, 1999; Ganeshram et al., 2000). The sedimentary $\delta^{15}N$ signatures reflect denitrification changes in intermediate waters (e.g., Altabet et al., 1999; Brandes et al., 1998; Ganeshram et al., 2000; Kessarkar et al., 2010, 2013). Thus, past changes in the OMZ intensity and water column denitrification have been inferred from sedimentary $\delta^{15}N$ with higher/lower values qualitatively indicating increases/decreases in denitrification intensity in the intermediate waters. The inferred changes have been related to variations in water mass composition, monsoon intensity, deep convective mixing, upwelling strength, and N_2 fixation (Agnihotri et al., 2003; Altabet et al., 1999; Banakar et al., 2005; Ganeshram et al., 2000; Gaye et al., 2018; Kao et al., 2015; Kessarkar et al., 2010, 2013; Pichevin et al., 2007; Reichart et al., 1998; Suthhof et al., 2001). These studies have mostly focused on glacial-interglacial time scales, including variations associated with the Dansgaard-Oeschger and Heinrich events in the North Atlantic. Higher-resolution Holocene studies by Agnihotri et al. (2003) and Naik et al. (2014) suggested an increase in denitrification linked to increased productivity from 10 to 2 ka BP and from 7 ka BP to the present, respectively. While these results from the Arabian Sea indicate an intensification of the OMZ during the Holocene (Agnihotri et al., 2003; Naik et al., 2014; Pichevin et al., 2007), rest of the world's oceans mostly experienced decrease in the extent and intensity of the OMZ (Deutsch et al., 2005). Most of the above studies have described the OMZ as a whole water column zone with the changing intensity related to processes like upwelling, convective mixing, or changes in inflowing water masses. It is not known if the vertical homogeneity of the OMZ varied during

the Holocene, which may be important for the potential relationship between the Holocene denitrification change and global atmospheric N_2O. Here we present high-resolution data from the sediment core SK148/55 (17°45'N, 70°52'E, 500-m water depth) located within the present-day OMZ at the lower boundary of the denitrifying zone (Figure 1). The $\delta^{15}N$ (indicating ventilation changes of the intermediate waters) and $\delta^{98}Mo$ (indicating bottom water oxygenation/anoxia) data document decoupled mesopelagic and bottom water (water in contact with sediment) oxygenation/ventilation changes during the Holocene. Our results show that the OMZ of the Arabian Sea did not always act as single homogenous zone but that parts of it could have been more oxygenated at times, which may have had implications for global atmospheric N_2O content.

2. Study Area

The Arabian Sea is semienclosed basin that is land locked in the north, east, and west. During the southwest monsoon (June–September) the intertropical convergence zone moves over the eastern Arabian Sea leading to high precipitation and runoff with low salinity surface waters occurring along the west coast of India. Rainfall on the landward side (in Ratnagir district) of core SK148/55 is high (average of 3,400 mm), which mainly occurs from June to September (http://hydro.imd.gov.in). Wind-driven surface currents flow clockwise during the southwest monsoon with upwelling centers observed off Arabia and Somalia and in the southeastern Arabian Sea (Qasim, 1977). The West India coastal current flows toward the south (Figure 1a), at the same time the West India Undercurrent (WIUC) moves northward extending up to 17°N and 200-m water depth with dissolved oxygen (O_2) contents in the core of the current being around 25 μM (Naqvi et al., 2006). During the northeast monsoon the surface currents move in anticlockwise direction (Figure 1a) with high productivity induced by convective mixing in the northern part of the basin. The OMZ located below 100-/150-m depth to a maximum of 1,200 m with O_2 below 0.5 ml/L (~22 M) that exists throughout the year (Sen Gupta & Naqvi, 1984; Wyrtki, 1971). The core of the OMZ that experiences denitrification consists of a mixture of high salinity water masses originating from the Persian Gulf and the Red Sea (Persian Gulf water and Red Sea Water) and lower salinity intermediate waters flowing in from the south (Sen Gupta & Naqvi, 1984, and references therein). The intermediate waters from the south (Subantarctic Mode Water/Indian Ocean Central Water) enter the Arabian Sea with higher oxygen contents that can be detected up to 17°N (Naqvi et al., 2006). There is also an intrusion of relatively oxygenated water along the western continental margin of India via the undercurrent (WIUC) during the southwest monsoon (Naqvi, 1991; Naqvi et al., 2006; Schott & McCreary, 2001; Shetye et al., 1994). It was believed earlier (Sen Gupta & Naqvi, 1984; Wyrtki, 1973) that the OMZ owes its existence to high productivity supported by upwelling during the southwest monsoon and convective mixing during the northeast monsoon and slow renewal of intermediate waters. However, it is now generally agreed that the ventilation of the OMZ is not sluggish; instead, the waters responsible for renewal have low O_2 contents (Naqvi, Yoshinari, Brandes, et al., 1998).

3. Methods

Gravity core SK148/55 was collected from 500-m water depth (Thamban et al., 2007), which is located close to the lower boundary of the perennial denitrification zone. The denitrification zone is characterized by high $\delta^{15}N$ of N_2O and NO_3^- (Figure 1) as reflected by seawater data from a nearby site (station SS3201 of Naqvi, Yoshinari, Jayakumar, et al., 1998). Laminations were observed throughout the core, and the chronology is based on seven accelerator mass spectrometry ^{14}C dates on *Globigerinoides ruber* (Thamban et al., 2007). The sedimentation rate varied from 0.4 to 1.83 mm/year (Figure 2).

The planktonic foraminiferal species *G. ruber* was selected for measurements of oxygen isotope composition of carbonate ($\delta^{18}O_C$). *G. ruber* tests were picked from 95 samples, cleaned ultrasonically, and analyzed for stable oxygen isotopes ($^{18}O/^{16}O$) on a Micromass IsoPrime Isotope Ratio Mass Spectrometer at the Geological Survey of Japan, Tsukuba. Replicate analysis of NBS-19 and internal laboratory standards revealed an external precision better than ±0.07‰.

Powdered bulk sediment samples (2 g) were treated with 1N HCl for the removal of $CaCO_3$ and were rinsed repeatedly with deionized water until the acid was completely removed and then dried in an oven at 60 °C. Weighed quantities (~20 mg) of dry, powdered samples filled into tin cups were analyzed for stable carbon and nitrogen isotopes using Finnigan Delta Plus isotope ratio mass spectrometer after combustion in a Flash 1112 EA elemental analyzer at the Centre for Marine Tropical Ecology, Bremen, Germany. The carbon and
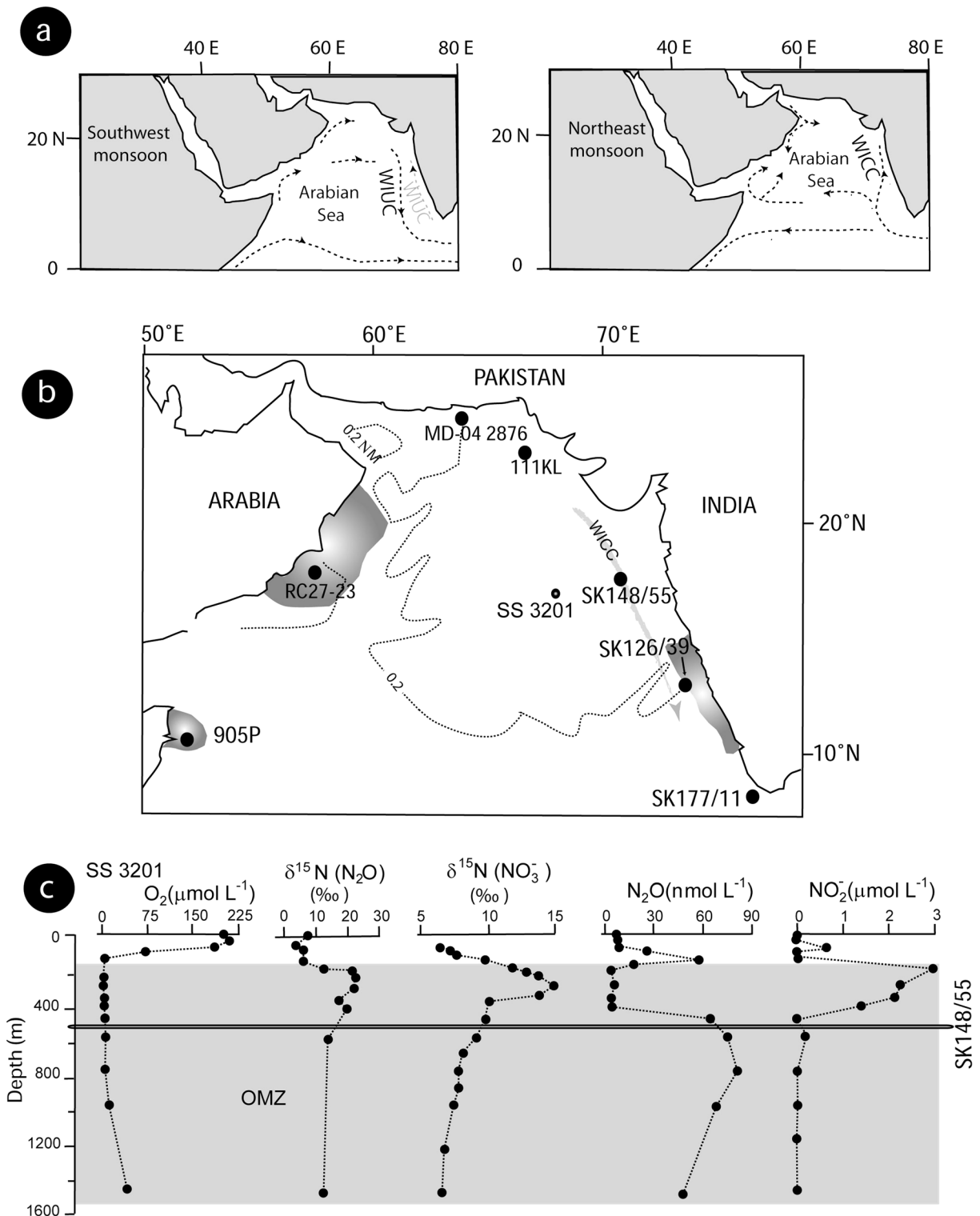
Figure 1. (a) Figure showing surface currents (black dotted lines) arrows are the direction of the currents: WICC = West Indian Coastal Current; WIUC = West Indian Undercurrent (Schott & McCreary, 2001. (b) Location of gravity cores (marked by solid circles) with respect to the denitrification zone (marked by the gray dotted line at $NO_2^- = 0.2$ μmol/L). The open circle is location SS3201 of the water column profiles; the core locations include SK148/55 (present study), 905P (Ivanochko et al., 2005), MD-04 2876 (Pichevin et al., 2007), 111KL (Suthhof et al., 2001), SK 126/39 (Kessarkar et al., 2010), and SK177/11 (Kao et al., 2015). The gray shaded areas indicate highly productive zones. (c) Water column profiles of O_2, $\delta^{15}N$ (N_2O), $\delta^{15}N$ (NO_3^-), N_2O, and NO_2^- above and within the OMZ; OMZ marked by gray shading; modified after Naqvi, 1991; Naqvi et al., 2003; Qasim, 1977). OMZ = oxygen minimum zone.
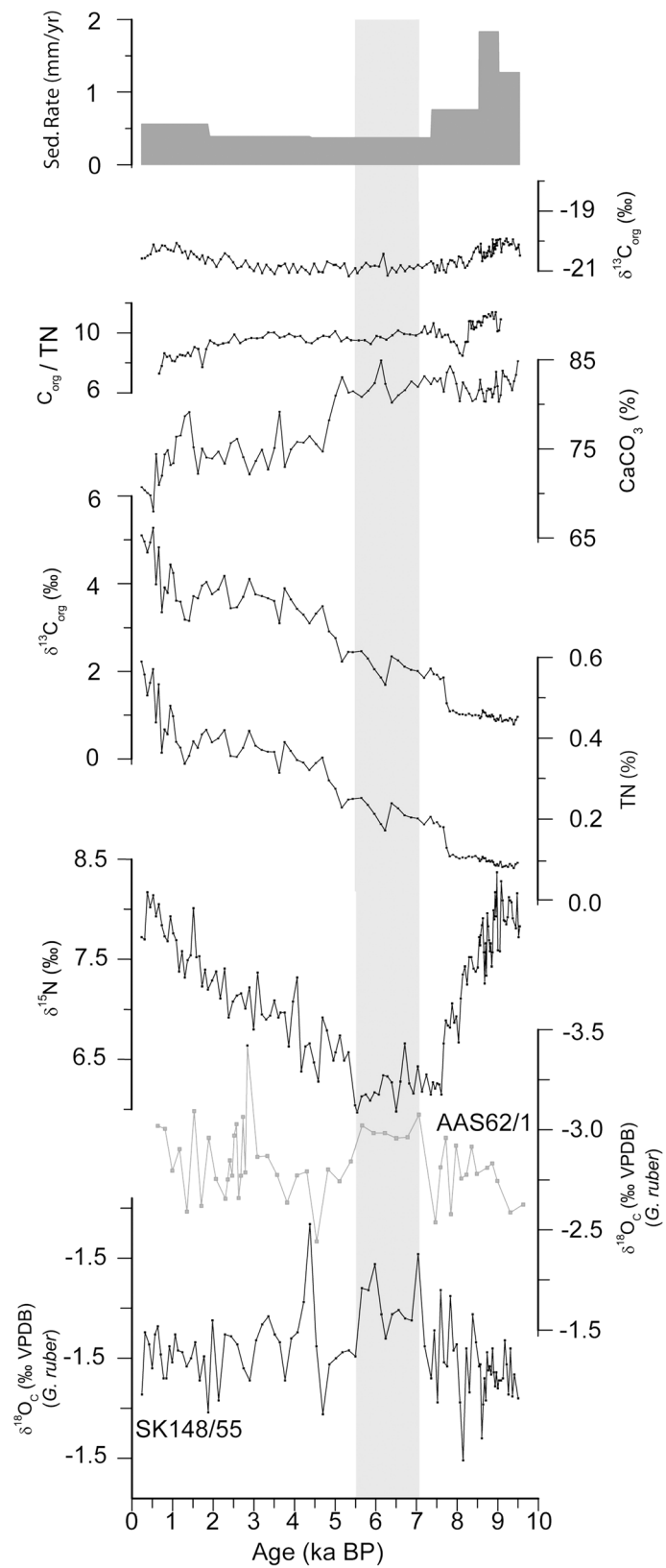
Figure 2. Stable oxygen isotope ($\delta^{18}O_C$) values (black—present study; gray—AAS62/1; Kessarkar et al., 2013), sediment nitrogen isotopes ($\delta^{15}N$), total nitrogen (TN), C_{org}, $CaCO_3$, C_{org}/TN, $\delta^{13}C_{org}$, and linear sedimentation rate: The vertical gray shaded area marks low denitrification.

nitrogen isotope ratios are expressed as per mil (‰) deviations from Pee Dee Belemnite and atmospheric N_2, respectively. Analytical precision based on duplicate analysis and internal standard measurement after every four samples was ±0.2‰ for $\delta^{15}N$ and ± 0.3‰ for $\delta^{13}C$. For calibration, the international reference standards IAEA N1 and N2 were used for $\delta^{15}N$ and U.S. Geological Survey (USGS) 24 and NBS 22 for $\delta^{13}C$. Two successive data points are separated by time periods ranging from 20 to 80 years.

For trace elemental analysis, samples were treated with 5:2.5:2.5:5-ml mixtures of concentrated $HClO_4$:HCl: HNO_3:HF and kept overnight on a hotplate at 100 °C. Subsequently, the samples were heated to 140 °C for 2 hr. Upon cooling the samples were treated with 1.5:1.5:3 ml of HCl:HNO_3:HF and again heated overnight at 140 °C. The temperature was increased to 170 °C the next day to dry the samples. This step was repeated until the sample was completely digested. The samples were then dissolved in 100 ml of 1M HNO_3 and the major elements were analyzed using a Seiko SPS 7800 Inductively coupled plasma atomic emission spectroscopy (ICP-AES) (Thamban et al., 2007). Minor and trace elements were determined using a HP 4500 ICP-MS at the Geological Survey of Japan, Tsukuba. Based on replicate measurements of rock standards of the Geological Survey of Japan (JR2, JA2, JB2, and JB1A), the measurement accuracies are estimated to be better than 5% (1 standard deviation, S.D.) for all trace elements and 1–2% for major elements.

For Mo isotopes, 500 mg of powdered sample was treated with 1M HCl to remove $CaCO_3$ and was subsequently dried down. Samples were then digested in a 2:2:4 ml HNO_3:HF:$HClO_4$ mixture at 180 °C overnight. This resulted in clear sample solutions, which were then dried down on the hot plate at 180 °C. To resolve instrument and laboratory mass fractionation of stable Mo isotopes a Mo double spike (^{100}Mo, ^{97}Mo) was added and data reduction subsequent to analysis was carried out following the procedures described in Siebert et al. (2001). Samples for Mo isotope analysis were purified using 2-ml cation exchange resin in 0.5M HCl (Biorad AG50W-X, 200–400 mesh) to remove iron and subsequently passed through 2 ml of anion exchange resin (Biorad AG 1x8, 200–400 mesh) in 4M HCl, and 2M HNO_3 to remove all other elements and to elute Mo. The samples were analyzed using a Nu instruments Multicollector-Inductively Coupled Plasma Mass Spectrometer (MC-ICPMS) at GEOMAR, Germany. The data are presented as $\delta^{98}Mo = [(^{98/95}Mo_{Sample}-^{98/95}Mo_{Standard})/^{98/95}Mo_{Standard}] \times 1{,}000$. All results are presented relative to the Alfa Aesar ICP standard solution (Specpure® #38791 (lot no. 011895D); for international comparison, NIST 3134 is 0.13‰ heavier than our in-house standard solution and we measured seawater at the established literature $\delta^{98}Mo$ value of 2.3 (Goldberg et al., 2013; Greber et al., 2012; Nägler et al., 2014). The external reproducibility of the in-house standard measurements was 0.05‰ (2 S.D.) during the measurement period. Reproducibility of USGS shale standard SDO-1 over the course of 2 years yielded a long-term reproducibility of 0.11‰. USGS standard MAG-1, a marine sediment, was digested twice and each digestion was analyzed twice in the course of these measurements yielding an average $\delta^{98}Mo$ of −0.2. Two samples were digested twice and analyzed in separate measurement sessions resulting in a reproducibility of 0.08‰ and 0.14‰ (2 S.D.), respectively. Total procedural blanks were at or below 3-ng Mo, while the measurements were performed at 100-ng Mo.

4. Results

4.1. Variations in $\delta^{18}O_C$

The $\delta^{18}O_C$ of *G. ruber* in the core SK148/55 exhibit an average value of −2.02‰ (range −2.7‰ to −1.5‰; Table S1 in the supporting information) over the past 9.5 ka (0.25 to 9.5 ka BP). The $\delta^{18}O_C$ for the period of time from 7 to 5.5 ka BP (average −2.3‰, range −2.5‰ to −2.1‰) is overall lighter than from 5.5 to 0.2 ka BP (average −2‰, range −2.7‰ to −1.7‰) and from 9.5 to 7 ka BP (average −1.9‰, range −2.3‰ to −1.5‰). Averaging data for each kiloyear shows that 5 to 6 ka and 6 to 7 ka periods are characterized by lighter $\delta^{18}O_C$ values of −2.22‰ and −2.52‰, respectively. From 9.5 to 7.5 ka BP the $\delta^{18}O$ fluctuates rapidly between lighter to heavier values, but from 7.5 to 4.7 ka the values show a more steady shift toward lighter and then to heavier values. Relatively light values with an average of −2.3‰ from 7 to 5.5 ka BP are comparable to the decrease in $\delta^{15}N$. There are three more steady changes observed around 4.3, 3.4, and 2.3 ka BP (Figure 2), but these occur at shorter time scales and/or with heavier values compared to those of 7 to 5.5 ka BP.

4.2. Variations in C_{org}, Total Nitrogen, Nitrogen, and Carbon Isotopes in the Sediments

The C_{org} concentrations range between 0.8% and 5.1%, with an average of 2.2%. The values are relatively low (0.8% to 1%; average of 0.9%) between 9.5 and 8.9 ka BP (early Holocene) and after that show a systematic
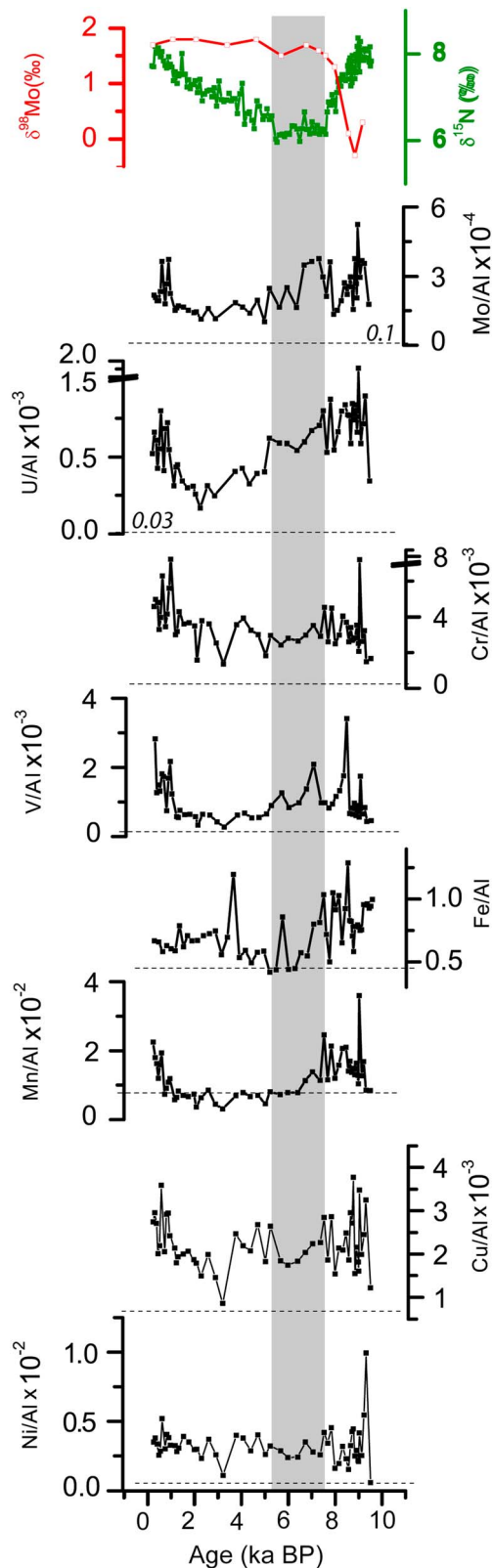
Figure 3. Temporal variations in Ni/Al, Cu/Al, Mn/Al, (Fe/Al; Thamban et al., 2007), V/Al, Cr/Al, Mo/Al, U/Al, $\delta^{15}N$, and $\delta^{98}Mo$ (open boxes). Dotted lines indicate Post-Archean Australian Shale values for the respective Al-normalized element. The gray shaded area marks low denitrification:

increase toward the core top. Total nitrogen (TN) content ranges between 0.08% to 0.59% with an average of 0.25%. Lower values of TN are observed during the early Holocene, while higher values occur toward the core top and exhibiting a trend similar to that of C_{org} (Figure 2). The C_{org}/TN ratio ranges between 8.6 and 10.3 (Figure 2), and C_{org} and TN show very high correlation coefficient ($R = 0.997$) with zero intercept of C_{org} on the negative axis of the TN (Figure S1). The $\delta^{15}N$ ranges from 6‰ to 8.4‰. From 9.5 to 7.6 ka BP the $\delta^{15}N$ values exhibit a marked decreasing trend. From 9.5 to 8.4 ka $\delta^{15}N$ exhibit an average value of 7.8‰ and while from 8.4 to 7.6 ka with an average value of 7.0‰. Later from 7.6 to 5.4 ka BP $\delta^{15}N$ does not show much variation with the values ranging between 6‰ and 6.7‰ (average of 6.2‰). From 5.4 to 0.2 ka BP $\delta^{15}N$ values again exhibit increasing trend reaching values up to 8.2‰. The $\delta^{15}N$ versus TN graph (Figure S2) does not show any significant correlation ($R = 0.053$). The $\delta^{13}C_{org}$ ranges between -21.1‰ and -19.9‰ and does only show small changes. The average values for $\delta^{13}C_{org}$ are -20.4‰ (9.5 to 7.6 ka BP), -20.9‰ (7.6 to 5.4 ka BP), and -20.7‰ (5.4. to 0.2 ka BP), and they are associated, respectively, with decreasing, stable, and increasing $\delta^{15}N$ values.

4.3. Elemental Concentrations and Molybdenum Isotopes in Sediments

The average elemental concentrations followed the sequence Mn > Ni > Cr > Cu > V > U > Mo. The metal contents of the sediments are expected to be controlled by a combination of lithogenic inputs, productivity, and the redox environment. At the first glance concentrations of most elements (Table S2) are much lower than the lithogenic background as inferred from Post-Archean Australian Shale (PAAS) values, except Mo, U, and Ni, which are enriched over PAAS in some sections of the core. However, because the sediments consist of >70% of biogenic carbon ($CaCO_3 + C_{org}$), lowered elemental concentrations with respect to PAAS are mainly caused by dilution. Elemental data were thus normalized to the Al content of the respective sample. Aluminum is of lithogenic origin, and the normalization would remove the source effect (Tribovillard et al., 2006), as well as dilution with biogenic carbonate. These Al-normalized values are used for further discussion (Figure 3). Al-normalized values of Ni, Cu, V, Cr, and U are much higher than the Al-normalized values of the PAAS elements, whereas Mn and Fe show lower concentrations in some parts of the core (Figure 3). The ratios are higher during the period 9.5–8.5 ka BP (Table S2) than during 7.5 to 5.6 ka BP. Low $\delta^{15}N$ during the period of time from 7.5 to 5.6 ka BP is associated with a decreasing trend of Mn/Al, Fe/Al, Mo/Al, and U/Al with not much variation in Cr/Al. The $\delta^{98}Mo$ in the core varied between -0.35‰ and 1.85‰ with lighter values averaging -0.02‰ (-0.4‰ to 0.3‰) between 9.8 and 8.5 ka BP followed by an increase from -0.1‰ to 1.7‰ between 8.5 to 7.3 ka BP and remaining relatively constant (from 1.55‰ to 1.85‰) since 7.3 ka BP.

5. Discussion

The observed $\delta^{18}O_C$ values of *G. ruber* varied between -2.7‰ and -1.5‰ over the past 9.5 kyr (Figure 2) with the difference between the beginning and the end of the record (9.5 and 0.3 ka BP) being ~0.3‰. This difference is comparable to the value (0.36‰) ascribed to sea level change during

this period (Waelbroeck et al., 2002). In contrast, the observed oscillations within the Holocene are large, in particular, between 8 and 4 ka BP. Between 7 and 5.5 ka (around the mid-Holocene) significantly lower $\delta^{18}O_C$ values (average of $-2.3‰$) are observed, which are followed by an increase of 0.8‰ within a period of 1.4 kyr until 4.6 ka. Subsequently, a rapid decrease by 0.9‰ within 0.3 kyr (4.6 to 4.3 ka) occurred followed again by a decrease of 0.8‰ within 0.6 kyr (4.3 to 3.7 ka). The $\delta^{18}O_C$ is determined by the combination of temperature and salinity of the water in which the foraminifera shells are formed, and it can also be affected by evaporation and precipitation (Conroy et al., 2014). About a 0.21‰ to 0.23‰ change in $\delta^{18}O_C$ is expected per degree temperature and 0.5‰ per unit salinity (Ravelo & Hillaire-Marcel, 2007). The sea surface temperature (SST) change expected for the entire Holocene is about 1.3 °C based on artificial neural network (Naidu & Malmgren, 2005) and 2.4 °C based on Mg/Ca-derived (from *G. ruber*) temperature (Saraswat et al., 2016). Therefore, a $\delta^{18}O_C$ change of 0.8 to 0.9 (corresponding to an SST change of 3.8 to 4.3 °C) within a period of 300 to 1,400 years is unrealistically high. However, the observed $\delta^{18}O_C$ change of 0.8 to 0.9 would correspond to a salinity change of 1.6 to 1.8 psu. Therefore, the lower $\delta^{18}O_C$ observed in the core of our study was most likely caused by reduced salinity (in addition to temperature) as a consequence of climatically driven precipitation changes as the core location is greatly affected by land runoff and precipitation during summer monsoon (Kessarkar et al., 2013). This is supported by results of Dahl and Oppo (2006), Kessarkar et al. (2013), and Saraswat et al. (2016). Therefore, the lower $\delta^{18}O_C$ signatures in our core reflect higher monsoon-induced precipitation/runoff between 8 to 4 ka BP that was most pronounced between 7 and 5.6 ka BP.

5.1. Changes in Denitrification During the Holocene

Considering that sea level rose by only 45 m over the past 9.5 kyr (Fairbanks, 1989), the sediments of our core (collected at 500-m depth) were deposited within the depth range of the OMZ (Figure 1b).

5.1.1. Sedimentary $\delta^{15}N$ and Its Controlling Factors

The $\delta^{15}N$ of organic matter in the core ranges between 6‰ and 8.4‰. The average $\delta^{15}N$ value of NO_3^- in the open ocean is ~4.7‰ (Sigman et al., 1997). The $\delta^{15}N$ of $NO3^-$ is much higher (e.g., ~15‰, Figure 1c) within the denitrification zones such as the Arabian Sea (Altabet et al., 1999; Naqvi, 1991; Suthof et al., 2001). As this isotopically heavy NO_3^- is brought up from the OMZ into the surface layer by upwelling/vertical mixing, it results in the production of organic matter that is enriched in ^{15}N and this signature gets preserved in the underlying sediments through sinking particles. In the Arabian Sea $\delta^{15}N$ values range between 4.7‰ and 8.8‰ for the settling particles and 9.2‰ and 11‰ for sediments (Schäfer & Ittekkot, 1995; Suthhof et al., 2001). These $\delta^{15}N$ values may partly be lowered by contributions of terrestrial organic matter that has a value of ~2‰ (Peters et al., 1978; Sweeney & Kaplan, 1980). The $\delta^{13}C$ values of organic material in the core range from $-21.1‰$ to $-19.4‰$, and C_{org}/TN is between 8.6 and 10.3, which is within the general range of marine organic matter in the Arabian Sea. Therefore, the organic matter in the core is dominantly of marine origin and the recorded $\delta^{15}N$ signatures originate from marine organic matter. Early diagenesis in the sediments can lead to elevated $\delta^{15}N$ values by as much as 4‰, but this mainly occurs in low organic-poor deep-sea sediments (Altabet & Francois, 1994). Our core is characterized by relatively high C_{org} contents (0.8% to 5.1%) of productive continental margin settings where diagenetic shift in $\delta^{15}N$ is small (Altabet et al., 1999; Pride et al., 1999). If influenced by diagenesis, one would expect a continuous increase to higher $\delta^{15}N$ values with depth, associated with low C_{org} and TN, which is not observed. However, we cannot rule out the possibility of minor diagenetic effects during the early Holocene (Figure 2) associated with low TN contents. In addition, incomplete utilization of nutrients in the surface waters can also result in higher $\delta^{15}N$ values (Altabet & Francois, 1994), which may be caused by iron (Fe) limitation (Naqvi et al., 2010). Similar $\delta^{15}N$ values of dissolved nitrate, the core top sediments (7.7‰), and sediment trap material (4.7–8.0‰; Schäfer & Ittekkot, 1995) support the suggestion of Altabet et al. (1999) and Suthhof et al. (2001) that on an annual basis NO_3^- gets completely utilized by the phytoplankton and incomplete utilization would not contribute to the observed $\delta^{15}N$ changes in our core. Enrichment in $\delta^{15}N$ (Figure 2 and Table S1) values can be caused by entrainment into the surface layer of waters enriched in $^{15}NO_3^-$ from the denitrification zone, which is then taken up by phytoplankton resulting in elevated $\delta^{15}N$ values in the organic matter that is ultimately transported to the sediments (Altabet et al., 1995, 2002, 1999; Ganeshram et al., 2000). Therefore, $\delta^{15}N$ (Figure 2 and Table S1) values ranging between 6‰ and 8.4‰ are suggested to be mainly a consequence of changes of denitrification intensity in the intermediate waters.

5.1.2. Changes in Sea Surface Productivity and Denitrification

High δ^{15}N values (7.7‰, Figure 2) of sediments at ~9.5 ka BP and near the core top sediments indicate intense denitrification within the OMZ. It has been proposed that the δ^{15}N changes in the Arabian Sea are related to the variability of the summer monsoon, with more intense denitrification occurring during periods of intensified summer monsoon and vice versa (Altabet et al., 1999; Ganeshram et al., 2000). Our δ^{15}N data show that this relationship is more complex in detail. Low $\delta^{18}O_C$ values are observed during the mid-Holocene (7–5.5 ka BP, Figure 2) suggesting strong summer monsoon intensity that likely resulted in increased freshwater inputs to the eastern Arabian Sea (Kessarkar et al., 2013; Singh et al., 2006). However, the δ^{15}N values during the mid-Holocene (7.6 to 5.4 ka BP) were low (average of 6.2‰) indicating weaker denitrification (Figure 2). Increase or decrease in denitrification intensity is often attributed to increase or decrease in surface productivity based on C_{org} (Agnihotri et al., 2003; Naik et al., 2014). However, the fact that only 1–3% of the C_{org} produced in the surface waters ultimately reaches the bottom sediments calls for caution in the universal use of C_{org} and $CaCO_3$ as proxies. The distribution of C_{org} in the Arabian Sea is influenced by upwelling induced productivity (Calvert et al., 1995) justifying its use as a proxy of productivity (Agnihotri et al., 2003; Naik et al., 2014, and references therein). In our core C_{org} and $CaCO_3$ contents do not show significant variations related to the changes in denitrification (Figure 2). Instead, the C_{org} and TN profiles exhibit systematic increases from 9.5 ka BP to the core top. High values of δ^{15}N at 9.5 ka BP indicate vigorous denitrification similar to the today (core top). But the high δ^{15}N at 9.5 ka BP is associated with low C_{org} contents (Figure 2) unlike the high core top δ^{15}N values, found with high C_{org} contents. Moreover, reduced denitrification appears to have been weaker during the mid-Holocene despite the relatively high C_{org} content (1.7% to 2.5%). Therefore, changes in C_{org} content that mainly reflected surface productivity cannot always be the only factor driving variations in denitrification intensity in the water column. Presently, the zones of the highest productivity (Figure 1a gray area) are not associated with the most intense denitrifying conditions in the Arabian Sea (Naqvi, 1991).

5.1.3. Southwest Monsoon Strength, Ventilation of Intermediate Water, and Denitrification Intensity

Changes in productivity on shorter time scales inferred from time series sediment trap data from the Arabian Sea have shown that stronger summer monsoon is not always associated with higher productivity (Rixen et al., 1996). Apart from upwelling strong summer monsoon winds also transfer nutrient-poor waters from south of the equator, thus reducing surface productivity in the western Arabian Sea. The sediment trap data from the eastern Arabian Sea also show that highest wind speeds and lowest SSTs are not always associated with increases in the biogenic particle fluxes. Instead, increased amounts of organic material are transferred to the deep sea during summer monsoons of intermediate strength (Rixen et al., 1996). As discussed by Rixen et al. (1996) if nutrient-poor water were reaching the study area, we would expect lower C_{org} and $CaCO_3$ contents. However, the lack of a pronounced decrease in C_{org} and $CaCO_3$ (Figure 2) between 7.6 and 5.4 ka BP essentially rules out the possibility of enhanced advection of nutrient-poor water. Records of sedimentary δ^{15}N in the Arabian Sea covering longer periods of time (Altabet et al., 2002, 1999; Reichart et al., 1998; Suthhof et al., 2001) have reported weaker denitrification linked to strong winter monsoon arising from cooling in the North Atlantic region (Reichart et al., 1998). These results suggested that such periods were characterized by deep convective mixing leading to greater ventilation of subsurface waters in the Arabian Sea (Reichart et al., 1998). Suppressed denitrification has also been reported during colder periods (Heinrich events and Younger Dryas in the North Atlantic; Suthhof et al., 2001) and on millennial time scales (Pichevin et al., 2007) likely caused by enhanced advection of more oxygenated Antarctic Intermediate Water into the Arabian Sea. Similar conditions characterized by low δ^{15}N are inferred in present study, which indicate weaker denitrification during a time of stronger summer monsoons as inferred from low $\delta^{18}O_C$ signals and other published records (Azharuddin et al., 2016; Kessarkar et al., 2013; Saraswat et al., 2016). Weaker denitrification has also been inferred previously for times of stronger summer monsoon based on analysis of cores off Mangalore (Kessarkar et al., 2010, 2013). This was attributed to a more vigorous ventilation of subsurface waters by the poleward flowing undercurrent (WIUC) carrying more oxygenated waters just below the West Indian Coastal Current (Figure 1) along the western margin of India at depths between 100 and 250 m (Naqvi et al., 2006). This undercurrent may have extended to the depth of the present core location at 17°45′N during times of stronger monsoon thereby ventilating the intermediate layers. Although a decrease in δ^{15}N during the mid-Holocene (Figure S4) has also been observed in cores off the Oman margin (Altabet et al., 2002) and off Pakistan (Reichart et al., 1998; Suthhof et al., 2001), this low in δ^{15}N was not

discussed in detail in the above studies that focused on changes occurring on the glacial-interglacial time scales or on specific events (e.g., Heinrich events). Pichevin et al. (2007) studied δ^{15}N variability in a core from the eastern Arabian Sea off Pakistan and compared it to the δ^{15}N records from the western Arabian Sea (RC27-23; RC27-14; Altabet et al., 2002; 905; Ivanochko et al., 2005) and showed that the variations in the east and the west were decoupled. However, these authors also did not discuss the low mid-Holocene δ^{15}N observed in the cores off Oman (core RC27-23). A minimum in denitrification intensity during this time has also been reported from the southeastern Arabian Sea (Kessarkar & Rao, 2007) suggesting that a relaxation in denitrification occurred on a large spatial scale during the mid-Holocene in the Arabian Sea. The locations recording minimum δ^{15}N values during the mid-Holocene are found close to the boundary of the present-day denitrification zone (Figure 1b). The denitrification zone most probably contracted during the mid-Holocene probably responding to a more effective oxygenation of the OMZ and has since been undergoing an expansion. It is noted that the mid-Holocene minimum in δ^{15}N is not observed in core MD-04 2876 from 828-m water depth (Pichevin et al., 2007) at the northern boundary of the denitrification zone but more studies at shallower depths off Pakistan are required to confirm the absence of this feature.

The presence of an intense OMZ supporting denitrification makes the Arabian Sea a globally significant source of nitrous oxide (N_2O) to the atmosphere (Naqvi et al., 2000) accounting for an estimated 2–35% of the global oceanic source (Bange et al., 2001). Changes in Arabian Sea denitrification have been postulated to have contributed to variations in atmospheric N_2O (Agnihotri et al., 2006; Altabet et al., 1995; Pichevin et al., 2007) as recorded in polar ice cores, such as Dome C from Antarctica that revealed decreasing N_2O concentrations (Figure S4) during the early Holocene (Flückiger et al., 2002). However, this does not imply a direct cause and effect relationship, but instead that these signals may have had a common origin (e.g., decrease in Northern Hemisphere summer insolation (Berger & Loutre, 1991); Figure S4).

5.2. Differential Changes in the OMZ and Near-Bottom Waters

Core SK148/55 investigated here is located within the present-day core of the Arabian Sea OMZ and close to the lower boundary of the denitrification zone (Figure 1). In order to assess changes in the redox status of bottom waters at the time of sediment deposition during the past 9.5 ka BP, we have investigated the downcore distribution of trace elements and δ^{98}Mo signatures (e.g., Anbar, 2004; Siebert et al., 2003). We observe very high Cu/Al and Ni/Al ratios as compared to PAAS, which has been suggested to reflect high organic matter supply (Tribovillard et al., 2006) given that Ni and Cu behave as micronutrients and form complexes with organic matter (Böning et al., 2015; Tribovillard et al., 2006). Although Ni and Cu can also form authigenic sulfides and enrichment is therefore not necessarily linked to productivity (given that there can be sulfate reducing microenvironments), we argue that, in combination with C_{org} accumulation rates (Figure S3), these elements indicate high productivity.

Stronger denitrification (high δ^{15}N) during the period between ~ 9.5 and 8.5 ka BP is associated with more variable and on average elevated Mo/Al, U/Al Fe/Al, and Mn/Al ratios (Cu/Al, Ni/Al, V/Al, and Cr/Al show no overall enrichment or increased variability) as compared to the mid-Holocene (Figure 3). Vanadium, Cr, Mo, U, Mn, and Fe are redox sensitive elements, which display different geochemical behavior depending on the ambient redox state. Vanadium in oxygenated water is adsorbed on to Fe-Mn oxyhydroxides, whereas under anoxic condition it is reduced to vanadyland binds to chelating surface groups (e.g., Morford & Emerson, 1999). Chromium in oxygenated water is soluble but under anoxic conditions becomes adsorbed onto Fe-Mn oxyhydroxides or forms complexes with humic/fulvic acid and can be released during anaerobic remineralization of organic matter and diffuses into overlaying water during sediment compaction (e.g., Tribovillard et al., 2006, and references therein). Molybdenum is adsorbed on Mn-Fe oxyhydroxides under oxic conditions, whereas under reducing conditions authigenic enrichment takes place (Morford & Emerson, 1999). U is dissolved [U (IV)] in an oxic environment and does not get scavenged or reduced (e.g., Anderson et al., 1989). Instead, U is removed by diffusion from the water column into the sediment followed by reduction of U (VI) to U (IV) that is subsequently precipitated or adsorbed forming authigenic U (Morford & Emerson, 1999; Tribovillard et al., 2006), whereby changes in sedimentation rate and oxygen penetration affect its concentration (Crusius & Thomson, 2000).

The period from 9.5 to 8.5 ka BP is associated with high V/Al, Mo/Al, and U/Al ratios possibly indicating that these elements were enriched under highly reducing conditions. However, high V/Al, Mo/Al, and U/Al ratios

also coincide with enrichments of Mn and Fe in the same samples, which argues against strongly reducing conditions during deposition. Recently, Scholz et al. (2011, 2017) suggested that under oxic or oxygen depleted, but nonsulfidic bottom water conditions Mo can be enriched in sediments via a Mn and/or Fe shuttle process in specific settings like the Baltic Sea or the OMZ offshore Peru where the transition to anoxic conditions is located relatively close to the sediment-water interface. The early Holocene section of the core exhibits high C_{org} accumulation rates (though C_{org} content is relatively low, see below). Anoxic conditions in the sediment caused by decaying organic matter can explain the enrichment of the diffusive U and Cr, while Mo and V are likely dominated by adsorption and transport by Mn-Fe oxyhydroxides. These oxyhydroxides would then release Mo below the sediment-water interface and with Mn and Fe partly diffusing back into the oxygenated bottom water to *capture* more Mo resulting in the establishment of a shuttle mechanism. In addition, it is likely that the high sedimentation rate (1.27 to 1.87 mm/year; Figure 2) quickly buried these sediments separating them from the biodegradation and also overlaying waters. This may explain the apparently contradictory enrichment of Mn and Fe together with Mo, V, U, and Cr.

To test the model for element enrichment and bottom water conditions presented above, Mo isotope (δ^{98}Mo) analyses were carried out. The Mo isotopes show distinctive values for different redox conditions, namely, light (~−0.7‰) in oxic, heavy (~1.5‰) in anoxic environments and reach values similar to seawater (~2.3‰) in euxinic settings due to complete removal of Mo from the water column as sulfide (e.g., Arnold et al., 2004; Barling et al., 2001; Goldberg et al., 2012; Neubert et al., 2008; Poulson-Brucker et al., 2009, 2006; Siebert et al., 2006, 2003). These changes in δ^{98}Mo mainly arise from the following reasons: Mo is a conservative element and is uniformly distributed in the oceans due to a much longer residence time (440 kyr; Miller et al., 2011) than the global ocean mixing time. Present-day oxic sea water has a uniform δ^{98}Mo signature of 2.3‰ (e.g., Siebert et al., 2003). Under oxic conditions light Mo isotopes are preferentially removed by adsorption to Mn oxides. Wasylenki et al. (2011) suggest adsorption of Mo as polymolybdate complex on the surface of Mn minerals indicating that the observed Mo isotope fractionation is caused by a change in coordination between dissolved and adsorbed Mo species. In suboxic to anoxic environments a wide variety of Mo isotope values have been observed, which are thought to be dependent on a variety of factors such as availability of Mn and Fe, thiomolybdate formation, Fe speciation, and the operation of a transport shuttle mechanism versus diffusion (e.g., Dahl et al., 2010; Goldberg et al., 2009, 2012; Poulson-Brucker et al., 2009; Scholz et al., 2017; Siebert et al., 2006; see also above). However, many anoxic settings seem to have converged around an isotope composition around 1.5‰ (e.g., Poulson-Brucker et al., 2009; Siebert et al., 2006). In general, all sedimentary fluxes of Mo are isotopically light, with Mo sulfides being the lightest (Tossell et al., 2005). Both oxic and anoxic but not sulfidic sinks remove light Mo isotopes from seawater, leaving the remaining seawater heavy (2.3‰). In sulfidic and hydrographically restricted settings, Mo is thought to be scavenged quantitatively resulting in a close to seawater isotope composition in euxinic sediments (e.g., Arnold et al., 2004).

In our core δ^{98}Mo values within the Holocene systematically vary between −0.35‰ and 1.85‰ suggesting that these sediments have been deposited under oxic and suboxic/anoxic water conditions at different time periods. Lithogenic sediments at this site are reported to be mainly derived from the Deccan traps in the hinterland (Kessarkar et al., 2003; Thamban et al., 2007). Suspended particulate matter supplied by the Narmada River that is passing through these formations has an average δ^{98}Mo of −0.03 ± 0.2 accompanied by very low Mo concentrations of 512 ± 44 ng/g (Rahaman et al., 2014). Mo concentrations observed in the studied core (see Table S1 and Figure 3) are clearly elevated (Mo/Al average of 2.4×10^{-4}; PAAS 1.1×10^{-5}; Figure 3) suggesting that this is not a crustal signature and that Mo is essentially derived from the water column. Between 9.5 and 8.5 ka BP light δ^{98}Mo (−0.4‰ to 0.3‰, average of −0.02‰) are associated with high Mo/Al and high Mn/Al and high accumulation rates. These very light Mo isotope values suggest that Mo enrichment together with Mn enrichment in this period is likely due to the operation of a Mn shuttle and that bottom waters at this time were well oxygenated. Similar observations for Mo isotopes have been presented by Siebert et al. (2006), Poulson-Brucker et al. (2006, 2009), and Goldberg et al. (2009).

The subsequent increase in δ^{98}Mo from 0.1‰ to 1.6‰ between ~8.5 and 7.5 ka BP would then indicate a marked change in bottom water conditions. Scholz et al. (2017) found that Mo scavenging by a Fe shuttle mechanism under suboxic/anoxic bottom water conditions within the OMZ along the Peruvian margin resulted in isotope compositions of around 1.5‰ in the underlying sediments. These findings and
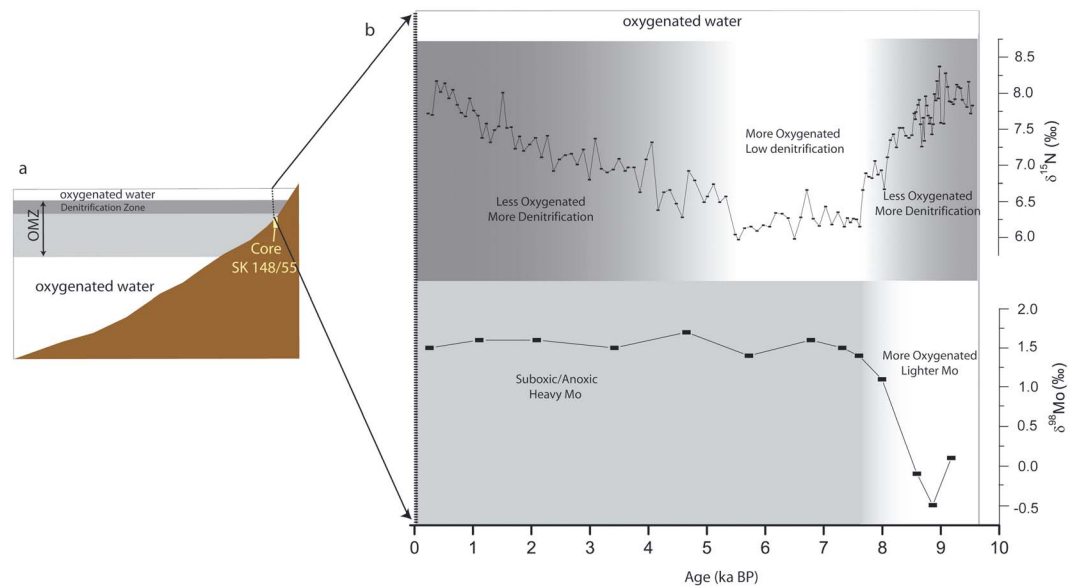
Figure 4. Schematic picture of water column oxygenation changes during the past 9.5 kyr. (a) Present-day water column and (b) core location changes in bottom water and intermediate water oxygenation inferred from the δ^{98}Mo and δ^{15}N records. OMZ = oxygen minimum zone.

previously published data (e.g., Poulson-Brucker et al., 2009) would suggest a change to anoxic/suboxic environment (Figure 3) of the bottom waters. These conditions stabilized between ~7.6 to 5.4 ka BP at uniform δ^{98}Mo values (1.55–1.75‰). At the same time enrichments of Fe and Mn decline while Mo, V, and U remain highly enriched despite of reduced sedimentation rates (Figures 2 and 3). Although the levels of enrichment of V/Al, Mo/Al, and U/Al indicate anoxic (Calvert & Pedersen, 1993; Tribovillard et al., 2006) or even euxinic conditions in the sediments during the mid-Holocene (Tribovillard et al., 2006 and references therein; Figure 3a), the Mo isotope signal does not indicate strongly reducing bottom water conditions (i.e., does not approach seawater). Scholz et al. (2017) have shown that very high Mo concentrations can be produced via a Fe shuttle mechanism under nonsulfidic conditions and Mo isotope values around 1.5‰ fit that interpretation. In addition, independent data have suggested that the Arabian Sea was low in oxygen but not sulfidic (Banse et al., 2014) during the present day. U becomes enriched in anoxic sediments by diffusion (Tribovillard et al., 2006, and references therein), which is reflected by U/Al far above the lithogenic background (Figure 3). We therefore suggest that bottom waters at the core site were better oxygenated in the early Holocene and changed to anoxic conditions around 7.5 ka BP. Subsequently, bottom waters remained anoxic.

5.3. Implications for the Water Mass Structure in the Arabian Sea During the Holocene

The period from ~9.5 to 8.5 ka BP is associated with lighter sedimentary Mo isotope signatures indicating oxygenated bottom waters, whereas high δ^{15}N indicates intense denitrification in the overlaying anoxic/suboxic water column (Figure 4). Subsequently from ~ 8.5 to 7.5 ka BP a decrease in δ^{15}N (indicating improved ventilation of the water column) was associated with increasing δ^{98}Mo values from −0.1‰ to 1.6‰ indicating shifting from oxic to anoxic/suboxic conditions. These findings imply that the OMZ as a whole was better oxygenated whereas the bottom waters at the study site were significantly less ventilated (Figure 4). These anoxic/suboxic bottom water conditions stabilized between ~7.6 and 5.4 ka BP supported by uniform δ^{98}Mo values (1.55–1.75‰). The δ^{15}N signature exhibits significantly lower values during the same time (7.6–5.4 ka BP) documenting more oxygenated, better ventilated conditions in the OMZ water column. Changes in organic carbon content and δ^{15}N in the Arabian Sea during early to mid-Holocene time have been related to more oxygenated conditions and reported in previous studies (e.g., Kao et al., 2015; Kessarkar & Rao, 2007; Kessarkar et al., 2010; Thamban et al., 2001). Kao et al. (2015) reported a decrease in δ^{15}N the southern Arabian Sea since 6 ka BP, in response to N_2 fixation and proposed that this was a local effect. The inferred weakening of denitrification toward the late Holocene (Ivanochko et al., 2005; Kao

et al., 2015) is, however, based on analyses of cores (905P and SK177/11; Figure 1a) located at a significant distance from the perennial denitrification zone and so it is possible that these cores may not have recorded the actual denitrification signals from the Arabian Sea during the Holocene period. It is also possible that there was a major reorganization of subsurface water masses in the Arabian Sea during the mid-Holocene in response to a decrease in Northern Hemisphere insolation (from 9 to 6–5 ka BP) that was accompanied by a stabilization of the sea level by 7 ka BP. This is expected to have affected advection of subsurface waters into the Arabian Sea both from outside (e.g., Subantarctic Mode Water) and within (Persian Gulf Water and Red Sea Water) this region. The δ^{15}N data suggest that the OMZ of the Arabian Sea was better ventilated/oxygenated during mid-Holocene (7.6–5.9 ka BP) resulting in a suppression of denitrification and that there has been a steady intensification/expansion of the OMZ since then. Considering the changes in the denitrification the most likely controlling processes are contractions and expansions of the perennial denitrification zone (Kessarkar et al., 2010; Naqvi, 1987, 1991). Changes in denitrification during the Holocene in intermediate waters and decoupled variations in bottom water conditions at present study site indicate variations in the vertical oxygen distribution within the OMZ. However, more detailed studies are required to identify the source of waters responsible for the better oxygenation parts/whole of the Arabian Sea OMZ during the mid-Holocene (Figure 4). Since 5.5 ka BP denitrification has continuously intensified suggesting reduced ventilation of OMZ associated with uniform Mo isotopes (average of 1.7‰) and consequently less oxygenated bottom waters.

6. Conclusions

The results of our study indicate that denitrification intensity in the Arabian Sea during the Holocene has not been controlled by upwelling intensity and productivity alone. During the early Holocene period (between 9.5 and 8 ka), pelagic denitrification was strong, but it probably occurred within a thinner upper layer as bottom waters at our coring site were better oxygenated as evident from light Mo isotope signatures. Denitrification weakened substantially during the mid-Holocene (7.6–5.4 ka BP), most likely in response to better ventilation of the OMZ at that time. This phase of weak denitrification was associated with a stronger summer monsoon and low N_2O levels in the atmosphere. We propose that a reorganization of subsurface water mass circulation was probably responsible for the weakening of Arabian Sea denitrification during the mid-Holocene. The bottom waters at the study site turned anoxic by ~7.5 ka BP, whereas the overlying water only changed to a less oxygenated state at ~5.5 ka BP and have since experienced a continuous intensification of denitrification.

References

Agnihotri, R., Altabet, M. A., & Herbert, T. D. (2006). Influence of marine denitrification on atmospheric N_2O variability during the Holocene. *Geophysical Research Letters*, *33*, L13704. https://doi.org/10.1029/2006GL025864

Agnihotri, R., Bhattacharya, S. K., Sarin, M. M., & Somayajulu, B. L. K. (2003). Changes in surface productivity and subsurface denitrification during the Holocene: A multiproxy study from the eastern Arabian Sea. *Holocene*, *13*(5), 701–713. https://doi.org/10.1191/0959683603hl656rp

Altabet, M. A., & Francois, R. (1994). Sedimentary nitrogen isotopic ratio as recorded for surface ocean nitrate utilization. *Global Biogeochemical Cycles*, *8*, 103–116. https://doi.org/10.1029/93GB03396

Altabet, M. A., Francois, R., Murray, D. W., & Prell, W. L. (1995). Climate-related variations in denitrification in the Arabian Sea from sediment $^{15}N/^{14}N$ ratios. *Nature*, *373*(6514), 506–509. https://doi.org/10.1038/373506a0

Altabet, M. A., Higginson, M. J., & Murray, D. W. (2002). The effect of millennial-scale changes in Arabian Sea denitrification on atmospheric CO_2. *Nature*, *415*(6868), 159–162. https://doi.org/10.1038/415159a

Altabet, M. A., Murray, D. W., & Prell, W. L. (1999). Climatically linked oscillations in Arabian Sea denitrification over the past 1 m.y.: Implications for the marine N cycle. *Paleoceanography*, *4*, 732–743. https://doi.org/10.1029/1999PA900035

Anbar, A. D. (2004). Molybdenum stable isotopes: Observations, interpretations and directions. *Reviews in Mineralogy and Geochemistry*, *55*(1), 429–454. https://doi.org/10.2138/gsrmg.55.1.429

Anderson, R. F., Fleisher, M. Q., & LeHuray, A. P. (1989). Concentration, oxidation state and particulate flux of uranium in the Black Sea. *Geochimica et Cosmochimica Acta*, *53*(9), 2215–2224. https://doi.org/10.1016/0016-7037(89)90345-1

Arnold, G. L., Anbar, A. D., Barling, J., & Lyons, T. W. (2004). Molybdenum isotope evidence for widespread anoxia in mid-Proterozoic oceans. *Science*, *304*(5667), 87–90. https://doi.org/10.1126/science.1091785

Azharuddin, S., Govil, P., Singh, A. D., Mishra, R., Agrawal, S., Tiwari, A. K., & Kumar, K. (2016). Monsoon-influenced variations in Productivity and lithogenic flux along offshore saurashtra, NE Arabian Sea during The Holocene and Younger Dryas: Amulti-proxy approach. *Palaeogeography, Palaeoclimatology, Palaeoecology*, *483*, 136–146. https://doi.org/10.1016/j.palaeo.2016.11.018

Banakar, V. K., Oba, T., Chodankar, A. R., Kuramoto, T., Yamamoto, M., & Minagawa, M. (2005). Monsoon related changes in sea surface productivity and water column denitrification in the Eastern Arabian Sea during the last glacial cycle. *Marine Geology*, *219*(2-3), 99–108. https://doi.org/10.1016/j.margeo.2005.05.004

Bange, H. W., Andreae, M. O., Lal, S., Law, C. S., Naqvi, S. W. A., Patra, P. K., et al. (2001). Nitrous oxide emissions from the Arabian Sea: A synthesis. *Atmospheric Chemistry and Physics*, *1*(1), 61–71. https://doi.org/10.5194/acp-1-61-2001

Banse, K., Naqvi, S. W. A., Narvekar, P. V., Postel, J. R., & Jayakumar, D. A. (2014). Oxygen minimum zone of the open Arabian Sea: Variability of oxygen and nitrite from daily to decadal timescales. *Biogeosciences*, *11*(8), 2237–2261. https://doi.org/10.5194/bg-11-2237-2014

Barling, J., Arnold, G. L., & Anbar, A. D. (2001). Natural mass-dependent variations in the isotopic composition of molybdenum. *Earth and Planetary Science Letters*, *193*, 447–457.

Berger, A., & Loutre, M. F. (1991). Insolation values for the climate of the last 10 million years. *Quaternary Sciences Review*, *10*(4), 297–317.

Böning, P., Shaw, T., Katharina, P., & Brumsack, H.-J. (2015). Nickel as indicator of fresh organic matter in upwelling sediments. *Geochimica et Cosmochimica Acta*, *162*, 99–108. https://doi.org/10.1016/j.gca.2015.04.027

Brandes, J. A., Devol, A. H., Yoshinari, T., Jayakumar, D. A., & Naqvi, S. W. A. (1998). Isotopic composition of nitrate in the central Arabian Sea and eastern tropical North Pacific: A tracer for mixing and nitrogen cycles. *Limnology and Oceanography*, *43*(7), 1680–1689. https://doi.org/10.4319/lo.1998.43.7.1680

Calvert, S., & Pedersen, T. (1993). Geochemistry of recent oxic and anoxic marine sediments: Implications for the geological record. *Marine Geology*, *113*(1-2), 67–88. https://doi.org/10.1016/0025-3227(93)90150-T

Calvert, S. E., Pedersen, T. F., Naidu, P. D., & Von Stackelberg, U. (1995). On the organic carbon maximum on the continental slope of the eastern Arabian Sea. *Journal of Marine Research*, *53*(2), 269–296. https://doi.org/10.1357/0022240953213232

Codispoti, L. A., Brandes, J. A., Christensen, J. P., Devol, A. H., Naqvi, S. W. A., Paerl, H. W., & Yoshinari, T. (2001). The oceanic fixed nitrogen and nitrous oxide budgets: Moving targets as we enter the anthropocene? *Scientia Marina*, *65*(Suppl.2), 85–105. https://doi.org/10.3989/scimar.2001.65s285

Conroy, J. L., Cobb, K. M., Lynch-Stieglitz, J., & Plissar, P. J. (2014). Contrasts on the salinity-oxygen isotope relationship in the central tropical Pacific Ocean. *Marine Chemistry*, *161*, 26–33. https://doi.org/10.1016/j.marchem.2014.02.001

Crusius, J., & Thomson, J. (2000). Comparative behaviour of authigenic Re, Mo and U during reoxidation and subsequent long-term burial in marine sediments. *Geochimica et Cosmochimica Acta*, *64*(13), 2233–2242. https://doi.org/10.1016/S0016-7037(99)00433-0

Dahl, K. A., & Oppo, D. W. (2006). Sea surface temperature pattern reconstructions in the Arabian Sea. *Paleoceanography*, *21*, PA1014. https://doi.org/10.1029/2005PA001162

Dahl, T. W., Anbar, A. D., Gordon, G. W., Rosing, M. T., Frei, R., & Canfield, D. E. (2010). The behavior of molybdenum and its isotopes across the chemocline and in the sediments of sulfidic Lake Cadagno, Switzerland. *Geochimica et Cosmochimica Acta*, *74*(1), 144–163. https://doi.org/10.1016/j.gca.2009.09.018

Deutsch, C., Emerson, S., & Thompson, L. (2005). Fingerprints of climate change in North Pacific oxygen. *Geophysical Research Letters*, *32*, L16604. https://doi.org/10.1029/2005GL023190

Devol, A. H., Uhlenhopp, A. G., Naqvi, S. W. A., Brandes, J. A., Jayakumar, A., Naik, H., et al. (2006). Denitrification rates and excess nitrogen gas concentrations in the Arabian Sea oxygen deficient zone. *Deep Sea Research*, *53*(9), 1533–1547. https://doi.org/10.1016/j.dsr.2006.07.005

Fairbanks, R. (1989). A 17,000 year glacio-eustatic sea level record: Influence of glacial melting rates on the Younger Dryas event and deep-ocean circulation. *Nature*, *342*(6250), 637–642. https://doi.org/10.1038/342637a0

Flückiger, J., Monnin, E., Stauffer, B., Schwander, J., Stocker, T. F., Raynaud, J. C. D., & Barnola, J. M. (2002). High-resolution Holocene N_2O ice core record and its relationship with CH_4 and CO_2. *Global Biogeochemical Cycles*, *16*(1), 1010. https://doi.org/10.1029/2001GB001417

Ganeshram, R. S., Pedersen, T. F., Calvert, S. E., McNeill, G. W., & Fontugne, M. R. (2000). Glacial-intergalcial variability in denitrification in the world's oceans: Causes and consequences. *Paleoceanography*, *14*, 361–376. https://doi.org/10.1029/1999PA000422

Gaye, B., Böll, A., Segschneider, J., Burdanowitz, N., Emeis, K.-C., Ramaswamy, V., et al. (2018). Glacial–interglacial changes and Holocene variations in Arabian Sea denitrification. *Biogeosciences*, *15*, 507–527. https://doi.org/10.5194/bg-15-507-2018

Goldberg, T., Archer, C., Vance, D., & Poulton, S. W. (2009). Mo isotope fractionation during adsorption to Fe (oxyhydr)oxides. *Geochimica et Cosmochimica Acta*, *73*(21), 6502–6516. https://doi.org/10.1016/j.gca.2009.08.004

Goldberg, T., Archer, C., Vance, D., Thamdrup, B., McAnena, A., & Poulton, S. W. (2012). Controls on Mo isotope fractionations in a Mn-rich anoxic marine sediment, Gullmar Fjord, Sweden. *Chemical Geology*, *296*, 73–82. https://doi.org/10.1016/j.chemgeo.2011.12.020

Goldberg, T., Gordon, G., Izon, G., Archer, C., Pearce, C. R., McManus, J., et al. (2013). Resolution of inter-laboratory discrepancies in Mo isotope data: An intercalibration. *Journal of Analytical Atomic Spectrometry*, *28*(5), 724. https://doi.org/10.1039/c3ja30375f

Greber, N. D., Siebert, C., Nägler, T. F., & Pettke, T. (2012). $\delta^{98/95}$Mo values and molybdenum concentration data for NIST SRM 610, 612 and 3134: Towards a common protocol for reporting Mo data. *Geostandards and Geoanalytical Research*, *36*(3), 291–300. https://doi.org/10.1111/j.1751-908X.2012.00160.x

Ivanochko, T. S., Ganeshram, R. S., Brummer, G. A., Ganssen, G., Jung, S. J. A., Moreton, S. G., & Kroon, D. (2005). Variations in tropical convection as an amplifier of global climate change at the millennial scale. *Earth and Planetary Science Letters*, *235*(1-2), 302–314. https://doi.org/10.1016/j.epsl.2005.04.002

Kao, S. J., Wang, B. Y., Zheng, L. W., Selvaraj, K., Hsu, S. C., Sean Wan, X. H., et al. (2015). Spatiotemporal variations of nitrogen isotopic records in the Arabian Sea. *Biogeosciences*, *12*(1), 1–14. https://doi.org/10.5194/bg-12-1-2015

Kessarkar, P. M., & Rao, V. P. (2007). Organic carbon in sediments of the southwestern margin of India: Influence of productivity and monsoon variability during the Late Quaternary. *Journal of the Geological Society of India*, *69*, 42–52.

Kessarkar, P. M., Rao, V. P., Ahmad, S. M., & Anil Babu, G. (2003). Clay minerals and Sr-Nd isotopes of the sediment along the western margin of India and their implication for sediment provenance. *Marine Geology*, *202*(1-2), 55–69. https://doi.org/10.1016/S0025-3227(03)00240-8

Kessarkar, P. M., Rao, V. P., Naqvi, S. W. A., Chivas, A. R., & Saino, T. (2010). Fluctuations in productivity and denitrification in the southeastern Arabian Sea during the late quaternary. *Current Science*, *99*, 485–491.

Kessarkar, P. M., Rao, V. P., Naqvi, S. W. A., & Karapurkar, S. G. (2013). Variation in the Indian summer monsoon intensity during the Bolling-Allerod and Holocene. *Paleoceanography*, *28*, 413–425. https://doi.org/10.1002/palo.20040

Miller, C. A., Peucker-Ehrenbrink, B., Walker, B. D., & Marcantonio, F. (2011). Re-assessing the surface cycling of molybdenum and rhenim. *Geochimica et Cosmochimica Acta*, *75*(22), 7146–7179. https://doi.org/10.1016/j.gca.2011.09.005

Morford, L. M., & Emerson, S. (1999). The geochemistry of redox sensitive trace metals in sediments. *Geochimica et Cosmochimica Acta*, *63*(11-12), 1735–1750. https://doi.org/10.1016/S0016-7037(99)00126-X

Nägler, T. F., Anbar, A. D., Archer, C., Goldberg, T., Gordon, F. W., Greber, N. D., et al. (2014). Proposal for an international molybdenum isotope measurement standard and data representation. *Geostandards and Geoanalytical Research*, *38*, 149–151. https://doi.org/10.1111/j.1751-908X.2013.00275.x

Naidu, P. D., & Malmgren, B. A. (2005). Seasonal sea surface temperature contrast between the Holocene and last glacial period in the western Arabian Sea (Ocean Drilling Project Site 723A): Modulated by monsoon upwelling. *Paleoceanography*, *20*, PA1004. https://doi.org/10.1029/2004PA001078

Naik, S. S., Godad, S. P., Naidu, P. D., Tiwari, M., & Paropkari, A. L. (2014). Early- to late-Holocene contrast in productivity, OMZ intensity and calcite dissolution in the eastern Arabian Sea. *Holocene*, *24*(6), 749–755.

Naqvi, S. W. A. (1987). Some aspects of the oxygen-deficient conditions and denitrification in the Arabian Sea. *Journal of Marine Research*, *45*, 1049–1072.

Naqvi, S. W. A. (1991). Geographical extent of denitrification in the Arabian Sea in relation to some physical processes. *Oceanologica Acta*, *14*, 281–290.

Naqvi, S. W. A., Jayakumar, D. A., Narvekar, R. V., Naik, H., Sarma, V. V. S. S., D'Souza, W., et al. (2000). Increased marine production of N_2O due to intensifying anoxia on the Indian continental shelf. *Nature*, *408*(6810), 346–349. https://doi.org/10.1038/35042551

Naqvi, S. W. A., Moffett, J. W., Gauns, M., Narvekar, P. V., Pratihary, A. K., Naik, H., et al. (2010). The Arabian Sea as a high-nutrient, low-chlorophyll region during the late southwest monsoon. *Biogeosciences*, *7*(7), 2091–2100. https://doi.org/10.5194/bg-7-2091-2010

Naqvi, S. W. A., Naik, H., & Narvekar, P. V. (2003). The Arabian Sea. In K. Black & G. Shimmield (Eds.), *Biogeochemistry of marine systems* (pp. 156–206). Oxford: Blackwell.

Naqvi, S. W. A., Naik, H., Pratihary, A. K., DeSouza, W., Narvekar, P. V., Jayakumar, D. A., et al. (2006). Coastal versus open-ocean denitrification in the Arabian Sea. *Biogeosciences*, *3*(4), 621–633. https://doi.org/10.5194/bg-3-621-2006

Naqvi, S. W. A., Yoshinari, T., Brandes, J. A., Devol, A. H., Jayakumar, D. A., Narvekar, P. V., et al. (1998). Nitrogen isotopic studies in the suboxic Arabian Sea. *Proceedings of the Indiana Academy of Sciences*, *107*(4), 367–378.

Naqvi, S. W. A., Yoshinari, T., Jayakumar, D. A., Altabet, M. A., Narvekar, R. V., Devol, A. H., et al. (1998). Budgetary and biogeochemical implications of N_2O isotope signatures in the Arabian Sea. *Nature*, *394*(6692), 462–464. https://doi.org/10.1038/28828

Neubert, N., Nägler, T. F., & Böttcher, M. E. (2008). Sulfidity controls molybdenum isotope fractionation into euxinic sediments: Evidence from the modern Black Sea. *Geology*, *36*(10), 775–778. https://doi.org/10.1130/G24959A.1

Peters, K. E., Sweeney, R. E., & Kaplan, I. R. (1978). Correlation of carbon and nitrogen stable isotope ratios in sedimentary organic matter. *Limnology and Oceanography*, *23*(4), 598–604. https://doi.org/10.4319/lo.1978.23.4.0598

Pichevin, L., Bard, E., Martinez, P., & Billy, I. (2007). Evidence of ventilation changes in the Arabian Sea during the last Quaternary: Implication for denitrification and nitrous oxide emission. *Global Biogeochemical Cycles*, *21*, GB4008. https://doi.org/10.1029/2006GB002852

Poulson-Brucker, R. L., McManus, J., Severmann, S., & Berelson, W. M. (2009). Molybdenum behavior during early diagenesis: Insights from Mo isotopes. *Geochemistry, Geophysics, Geosystems*, *10*, Q06010. https://doi.org/10.1029/2008GC002180

Poulson-Brucker, R. L., Siebert, C., McManus, J., & Berelson, W. M. (2006). Authigenic molybdenum isotope signatures in marine sediments. *Geology*, *34*(8), 617–620. https://doi.org/10.1130/G22485.1

Pride, C., Thunell, R., Sigman, D., Keigwin, L., Altabet, M., & Tappa, E. (1999). Nitrogen isotopic variations in the Gulf of California since the last degalciation: Response to global climate change. *Paleoceanography*, *14*, 397–409. https://doi.org/10.1029/1999PA900004

Qasim, S. Z. (1977). Biological productivity of the Indian Ocean. *Indian Journal of Marine Science*, *6*, 122–137.

Rahaman, W., Goswami, V., Singh, S. K., & Rai, V. K. (2014). Molybdenum isotopes in two Indian estuaries: Mixing characteristics and input to oceans. *Geochimica et Cosmochimica Acta*, *141*, 407–422. https://doi.org/10.1016/j.gca.2014.06.027

Ravelo, A. C., & Hillaire-Marcel, C. (2007). The use of oxygen and carbon isotopes of foraminifera in paleoceanography. In C. Hillaire-Marcel, & A. de Vernal (Eds.), *Proxies in Late Cenozoic paleoceanography*, (pp. 735–764). Amsterdam: Elsevier.

Reichart, G. J., Lourens, L. J., & Zachariasse, W. J. (1998). Temporal variability in the northern Arabian Sea oxygen minimum zone (OMZ) during the last 225,000 years. *Paleoceanography*, *13*, 607–621. https://doi.org/10.1029/98PA02203

Rixen, T., Haake, B., Ittekkot, V., Guptha, M. V. S., Nair, R. R., & Schlussel, P. (1996). Coupling between SW monsoon-related surface and deep ocean processes as discerned from continuous particle flux measurements and correlated satellite data. *Journal of Geophysical Research*, *101*, 28,569–28,582. https://doi.org/10.1029/96JC02420

Saraswat, R., Naik, D. K., Nigam, R., & Gaur, A. S. (2016). Timing, cause and consequences of mid-Holocene climate transition in the Arabian Sea. *Quaternary Research*, *86*(02), 162–169. https://doi.org/10.1016/j.yqres.2016.06.001

Schäfer, P., & Ittekkot, V. (1995). Isotopic biogeochemistry of nitrogen in the Northern Indian Ocean. *Mitteilungen aus dem Geologisch-Palaontologischen Institut der Universitat Hamburg*, *78*, 67–93.

Scholz, F., Hensen, C., Noffke, A., Rohde, A., Liebetrau, V., & Wallmann, K. (2011). Early diagenesis of redox-sensitive trace metals in the Peru upwelling area—Response to ENSO related oxygen fluctuations in the water column. *Geochimica et Cosmochimica Acta*, *75*(22), 7257–7276. https://doi.org/10.1016/j.gca.2011.08.007

Scholz, F., Siebert, S., Dale, A. W., & Frank, M. (2017). Intense molybdenum accumulation in sediments underneath nitrogenous water column and implications for the reconstruction of paleo-redox conditions based on molybdenum isotopes. *Geochimica et Cosmochimica Acta*, *213*, 400–417. https://doi.org/10.1016/j.gca.2017.06.048

Schott, A. F., & McCreary, J. (2001). The monsoon circulation of the Indian Ocean. *Progress in Oceanography*, *51*(1), 1–123. https://doi.org/10.1016/S0079-6611(01)00083-0

Sen Gupta, R., & Naqvi, S. W. A. (1984). Chemical oceanography of the Indian Ocean, north of the equator. *Deep Sea Research*, *31*(6-8), 671–706. https://doi.org/10.1016/0198-0149(84)90035-9

Shetye, S. R., Gouveia, A. D. & Shenoi S. S. C., (1994). Circulation and water masses of the Arabian Sea. Biochemistry of the Arabian Sea: Present information and gaps. Lal, D., *Proceedings of Indian Academy of Sciences (Earth Planet. Sci.)* (Vol. 103(2), pp. 107–123), Indian Acad. of Sci.; Bangalore; India.

Siebert, C., McManus, J., Bice, A., Poulson, R., & Berelson, W. M. (2006). Molybdenum isotope signatures in continental margin marine sediments. *Earth and Planetary Science Letters*, *241*(3-4), 723–733. https://doi.org/10.1016/j.epsl.2005.11.010

Siebert, C., Nagler, T. F., & Kramers, J. D. (2001). Determination of molybdenum isotope fractionation by double-spike multicollector inductively coupled plasma mass spectrometry. *Geochemistry, Geophysics, Geosystems*, *2*(7), 1032. https://doi.org/10.1029/2000GC000124

Siebert, C., Nagler, T. F., von Blanckenburg, F., & Kramers, J. D. (2003). Molybdenum isotope records as a potential new proxy for paleoceanography. *Earth and Planetary Science Letters*, *211*(1-2), 159–171. https://doi.org/10.1016/S0012-821X(03)00189-4

Sigman, D. M., Altabet, M. A., Michener, R., McCorkle, D. C., Fry, B., & Holmes, R. M. (1997). Natural abundance-level measurement of the nitrogen isotopic composition of oceanic nitrate: An adoption of the ammonia diffusion method. *Marine Chemistry*, *57*(3-4), 227–242. https://doi.org/10.1016/S0304-4203(97)00009-1

Singh, A. D., Kroon, D., & Ganeshram, R. S. (2006). Millennial scale variations in productivity and OMZ intensity in the eastern Arabian Sea. *Journal of the Geological Society of India*, *68*, 369–377.

Suthhof, A., Ittekkot, V., & Gaye-Haake, B. (2001). Millennial-scale oscillations of denitrification intensity in the Arabian Sea during the late Quaternary and its potential influence on atmospheric N_2O and global climate. *Global Biogeochemical Cycles*, *15*, 637–649. https://doi.org/10.1029/2000GB001337

Sweeney, R. E., & Kaplan, I. R. (1980). Natural abundances of ^{15}N as a source indicator for nearshore marine sedimentary and dissolved nitrogen. *Marine Chemistry*, *9*(2), 81–94. https://doi.org/10.1016/0304-4203(80)90062-6

Thamban, M., Kawahata, H., & Rao, V. P. (2007). Indian summer monsoon variability during the Holocene as recorded in sediments of the Arabian Sea: Timing and implications. *Journal of Oceanography*, *63*(6), 1009–1020. https://doi.org/10.1007/s10872-007-0084-8

Thamban, M., Rao, V. P., Schneider, R. R., & Grootes, P. M. (2001). Glacial to Holocene fluctuations in hydrography and productivity along the southwestern continental margin of India. *Palaeogeography, Palaeoclimatology, Palaeoecology*, *165*(1-2), 113–127. https://doi.org/10.1016/S0031-0182(00)00156-5

Tossell, J. A. (2005). Calculating the partitioning of the isotopes of Mo between oxidic and sulfidic species in aqueous solution. *Geochimica et Cosmochimica Acta*, *69*, 2981–2993.

Tribovillard, N., Algeo, T. J., Lyons, T., & Riboulleau, A. (2006). Trace metals as paleoredox and paleoproductivity proxies: An update. *Chemical Geology*, *232*(1-2), 12–32. https://doi.org/10.1016/j.chemgeo.2006.02.012

Waelbroeck, C., Labeyrie, L., Michel, E., Duplessy, J. C., McManus, J. F., Lambeck, K., et al. (2002). Sea-level and deep water temperature changes derived from benthonic foraminifera isotopic records. *Quaternary Science Reviews*, *21*(1-3), 295–305. https://doi.org/10.1016/S0277-3791(01)00101-9

Wasylenki, L. E., Weeks, C. L., Bargar, J. R., Spiro, R. G., Hein, J. R., & Anbar, A. D. (2011). The molecular mechanism of Mo isotope fractionation during adsorption to birnessite. *Geochimica et Cosmochimica Acta*, *75*(17), 5019–5031. https://doi.org/10.1016/j.gca.2011.06.020

Wyrtki, K. (1971). *Oceanographic atlas of the International Indian Ocean Expedition*, (p. 531). Washington, D. C: National Science Foundation.

Wyrtki, K. (1973). Physical Oceanography of the Indian Ocean. In B. Zeitzschel & S. A. Gerlach (Eds.), *The Biology of the Indian Ocean. Ecological Studies (Analysis and Synthesis)* (Vol. 3, pp. 18–36). Berlin: Springer.